Diffractive imaging of the dumbbell structure in silicon by spherical-aberration-corrected electron diffraction

Shigeyuki Morishita,[1] Jun Yamasaki,[2,a)] Keisuke Nakamura,[1] Takeharu Kato,[3] and Nobuo Tanaka[2]
[1]*Department of Crystalline Materials Science, Nagoya University, Furo-cho, Chikusa-ku, Nagoya 464-8603, Japan*
[2]*EcoTopia Science Institute, Nagoya University, Furo-cho, Chikusa-ku, Nagoya 464-8603, Japan*
[3]*Nanostructures Research Laboratory, Japan Fine Ceramics Center, 2-4-1 Mutsuno, Atsuta-ku, Nagoya 456-8587, Japan*

(Received 1 August 2008; accepted 29 September 2008; published online 3 November 2008)

The dumbbell structure in crystalline silicon as known with the separation of 0.136 nm has been reconstructed clearly by diffractive imaging using an electron beam. The spatial resolution in the result is estimated at about 0.1 nm. By utilizing the selected area diffraction technique in a spherical-aberration-corrected transmission electron microscope, one can reconstruct nanostructures with atomic resolution, even if they are not surrounded by empty space such as localized structures embedded in thin film samples. This means that the present method has a unique potential to expand the versatility of diffractive imaging by electron beams drastically. © *2008 American Institute of Physics*. [DOI: 10.1063/1.3003582]

Atomic structures of materials have been analyzed for a long time by using radiation scatterings. Generally, averaged structures such as unit cells in crystalline bulks are analyzed precisely by x-ray and neutron diffraction. On the other hand, localized structures and textures are analyzed by imaging methods such as transmission electron microscopy (TEM). In recent years, diffractive imaging has attracted attention as promising microscopy without imaging lenses, in which localized structures are reconstructed from diffraction intensity alone by iterative phase retrieval procedures.[1,2] Since the first experimental result in 1999,[3] this "lensless imaging" has been applied to some materials including biological ones by using coherent x-ray radiation,[4] in which the spatial resolution of about 7 nm has been achieved.[5]

Considering radii of Ewald spheres, electron beams are necessary to obtain projected atomic structures of materials. Spatial resolution in TEM images is, however, restricted by geometric and chromatic aberrations of imaging lenses, even now when the third-order spherical aberration (C_s) correctors have been developed.[6] Meanwhile, electron diffraction intensity is not influenced basically by lenses, apart from phase modulations. From the viewpoint of the lensless imaging, diffractive imaging using electron beams has a possibility for achieving higher resolution than the ordinary lens imaging. However, the ordinary electron diffractive imaging (EDI) is applicable only to nanomaterials surrounded by empty space as mentioned later. It might be one of the reasons for few achievements in EDI so far.[7–9] In this study, we propose a promising solution for the problem by using selected area diffraction in a C_s-corrected TEM.[10]

In the present experiments, crushed silicon mounted onto a microgrid is used. Electron diffraction patterns are recorded on imaging plates (IP) by using a 200 kV thermal field-emission TEM (JEOL: JEM-2100F) equipped with an imaging C_s-corrector (CEOS GmbH).

In the ordinary EDI, samples are illuminated by an electron probe more than 50 nm in diameter.[8,9] A field of view to be reconstructed must include empty space surrounding the samples, which is utilized for the constraint to retrieve the phases in reciprocal space. It means that the samples must be isolated in empty space such as nanotubes.[8,9] For example, weak scattering by an amorphous membrane supporting nanoparticles is not negligible for precise reconstruction. In cases of localized structures such as defects or interfaces embedded in thin films, the problem becomes much more serious. To avoid the problem, selected area diffraction might be effective because areas where electron beams are intercepted by the aperture can be used for the constraint.[7] For this purpose, a hole 240 nm in diameter has been opened in a copper thin plate by focused ion beams (FIB). When inserted in the conjugate plane of the objective lens, it works as an aperture selecting a nanometer-sized area in the object plane, which is much smaller than that selected by a conventional aperture in TEMs (more than 100 nm). Figures 1(a) and 1(b) show TEM images of the hole selecting vacuum and a part of crystalline silicon, respectively. The lengths of the major and minor axes of the slight elliptic hole are measured to be 3.1 and 2.6 nm by comparison with the {111} lattice fringes of silicon (d=0.313 nm).

It should be noted that selected area diffraction patterns generally include scattered waves coming from outside of an aperture hole. It is known in textbooks that the area selection error is caused by the C_s of the objective lens,[11] in other words, by the fact that diffraction in a TEM is not in lensless configuration in a true sense.[7] This effect becomes relatively remarkable in the case of the small hole used in the present study. Thus, using a C_s-corrected TEM is essential for obtaining a diffraction pattern from a well-defined area several nanometers in diameter with parallel illumination.[10] We refer to the technique as selected area nano-diffraction (SAND), distinguishing from conventional selected area diffraction. In the present experiments, the C_s value is corrected to less than 1.0 μm. The corresponding area selection error is within

a)Electronic mail: p47304a@nucc.cc.nagoya-u.ac.jp.

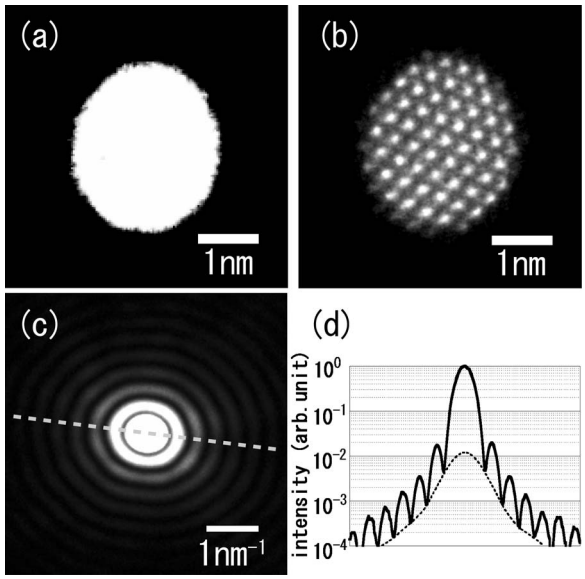

FIG. 1. TEM images of the aperture hole produced by FIB, which are selecting areas in vacuum (a) and in a silicon crystal (b). (c) SAND pattern corresponding to (a). (d) Intensity profile along the dotted line in (c).

0.05 nm in the frequency range used in the present study, which is negligible in the following analyses.

Figure 1(c) is a SAND pattern corresponding to Fig. 1(a), which shows intensity distribution resembling the Airy diffraction pattern from a circular pinhole. Figure 1(d) shows the intensity profile along the dotted line in Fig. 1(c). The profile consists of an oscillation part showing high spatial coherency of the electron beam inside the hole and a background part [a dotted line in Fig. 1(d)] caused by stray rays and/or scattering at the edge of the hole. In the present experiments, all the SAND patterns are recorded with beams more than 0.5 μm in diameter in the object plane to form such a coherent condition.

A SAND pattern from thin silicon along [110] is shown in Fig. 2(a), which consists of 1024×1024 pixels corresponding to 30.8×30.8 nm^{-1}. Sample drift during the exposure of 4.0 s is ignorable at an atomic level. After subtracting the background intensity in Fig. 1(d) and low-pass filtering for noise reduction, wave fields are reconstructed from the SAND intensity and a different random set of initial phases. At the beginning of the iterative process, an area with 1.1

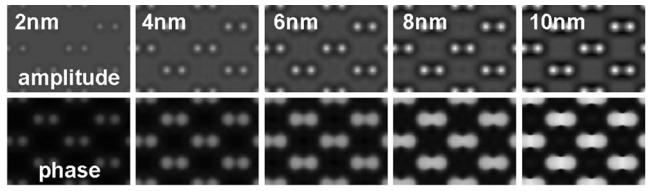

FIG. 3. Simulated wave fields below silicon crystals with different thicknesses denoted at the upper left in each image.

times larger diameter than the hole is defined as a "support" for real-space constraints. During the iteration, the shape of the support is updated automatically and repeatedly according to convergence of the wave fields toward the hole.[12] For the first 1000 cycles, hybrid input-output algorithm[2] with a convergence parameter $\beta=0.6$ is used, and for the following 500 cycles, error-reduction algorithm.[2] The non-negative constraint on the imaginary part is imposed for the inside of the support.[13]

One of the reconstructed wave fields is shown in Figs. 2(b) and 2(c), which are the amplitude and phase maps of 128×128 pixels around the hole. In the amplitude map, the alignment of atomic columns in silicon viewed from [110] is reconstructed in the hole. The dumbbell structure as known with the separation of 0.136 nm is resolved clearly. The inset of Fig. 2(b) is the Fourier power spectrum of the amplitude map in which the $4\bar{4}0$ spot corresponding to a resolution of 0.096 nm appears. The value is comparable to that in C_s-corrected TEM images by the instrument used in the present study, which is estimated at 0.1–0.11 nm by Young's fringes from an amorphous film. Despite the slight larger size of the initial support than the hole, the shape of the hole is reconstructed well. The axial lengths coincide with Fig. 1(a), namely, 3.1 and 2.6 nm. It is considered that the sufficient convergence to the shape of the hole comes from the pseudo Airy pattern convoluted on each diffraction spot in Fig. 2(a). It is known that this kind of "tight support" is an advantage for reliable reconstruction by diffractive imaging.[14] On the other hand, clear identification of each atomic column is rather difficult in the phase map, although the lattice fringes are seen. It should be noted that the random oscillation at the outside of the hole has no physical meaning because the phases are indeterminate due to the almost zero amplitude in the outside area.

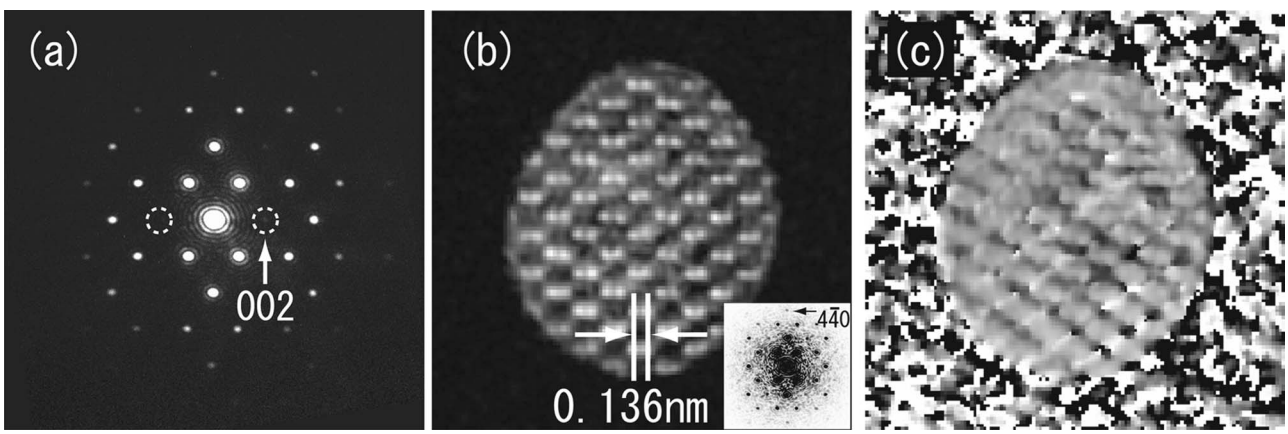

FIG. 2. (a) SAND pattern from a silicon crystal along [110]. The amplitude map (b) and the phase map (c) of a wave field reconstructed from (a). Fourier power spectrum of (b) is shown as the inset.

Figure 3 shows wave fields below silicon crystals that are calculated by the multislice method widely used for high-resolution TEM image simulations. Comparing intensity ratios of the 002 and direct spots in Fig. 2(a) and the simulations, the thickness of the area for Fig. 2(a) is estimated from 4 to 8 nm. In Fig. 2(b), bright dots less than 0.1 nm in diameter locate at atomic positions, which are reproduced well in Fig. 3. Regarding the random oscillation outside the hole in Fig. 2(c) as an extreme case, it is considered that small values of amplitudes in real space tend to cause indetermination in phases in the same pixels. Thus, the small values of the amplitudes except for the bright dots might cause the degradation in the phase map [Fig. 2(c)]. Considering also the lower resolution in the phase maps than the amplitude maps in Fig. 3, it is concluded that amplitude maps are suitable for structure analyses by diffractive imaging so far as atomic positions are concerned.

It is suspected that Fig. 2(a) includes elastic/inelastic additional backgrounds from the silicon and surface oxide layers, although we have subtracted carefully a background based on Fig. 1(d). As seen in Fig. 2(c) remarkably, also slight misorientation from the exact zone axis has influenced the results in terms of breakdown of symmetry. As the result of such experimental uncertainty, the unique amplitude map has not been reconstructed from 50 different initial phases. As criteria to identify proper results, we have exploited the following two important features in the Fourier power spectra of the amplitude maps in Fig. 3: (1) C_{2v} symmetry in intensity and (2) 002 and $00\bar{2}$ spots with significantly smaller intensity than 004 and $00\bar{4}$ spots. The second one is important for reproduction of the dumbbells. It has been confirmed that whenever the criteria are satisfied, atomic positions in the reconstructed amplitude map coincide intuitively with the actual ones such as Fig. 2(b). According to the criteria, the rate of the proper reconstruction is 22% at the present stage, which might be increased by improvements in iteration algorithms.

The reconstructed total field of view is 33.3 nm that is the inverse of the sampling frequency in Fig. 2(a). It is known that an oversampling ratio, an area ratio of a field of view to a support, has to be much more than 2.[5] In the present experiments, the ratio is more than 100 and high enough for the criterion. When using other larger holes, for example, selecting areas 30 nm in diameter for practical applications, the criterion is satisfied by increasing a camera length for recording and the number of pixels clipped from IP. It is known that an illumination probe with a spatial coherence length twice as large as a support is required for uniform reconstruction.[15,16] Almost uniform contrast of the silicon lattice in the hole [Fig. 2(b)] proves that the coherency in the present experiments is sufficiently high. When using other larger holes, the coherence length can be increased easily by enlarging the probe size. A nanometer-sized area can be selected also by a focused probe itself[17,18] instead of the present SAND technique. It should be noted, however, that the important advantage of the present method is the compatibility of the tight support and the coherent illumination all over the selected area.

In conclusion, we have developed a promising method for EDI in which a wave field is reconstructed from a selected area diffraction pattern in a C_s-corrected TEM. The spatial resolution of 0.1 nm has been achieved in the resultant amplitude map in which the dumbbells in a silicon crystal as known with the separation of 0.136 nm have been reconstructed clearly. The result means that one can reconstruct nanostructures with atomic resolution using EDI even if they are not surrounded by empty space such as localized structures embedded in thin film samples. It is concluded that the method developed in this study expands the versatility of EDI drastically.

We acknowledge Professor K. Gohara, Dr. O. Kamimura, Dr. Y. Nishino, Dr. E. Nishibori, and Dr. K. Saitoh for valuable comments and Dr. H. Sawada and Dr. T. Saito for their help. The present study was partly supported by MEXT KAKENHI (18029011) and JSPS KAKENHI (17201022).

[1] R. W. Gerchberg and W. O. Saxton, Optik (Stuttgart) **35**, 237 (1972).
[2] J. R. Fienup, Appl. Opt. **21**, 2758 (1982).
[3] J. Miao, P. Charalambous, J. Kirz, and D. Sayre, Nature (London) **400**, 342 (1999).
[4] Y. Takahashi, Y. Nishino, T. Ishikawa, and E. Matsubara, Appl. Phys. Lett. **90**, 184105 (2007).
[5] J. Miao, T. Ishikawa, E. H. Anderson, and K. O. Hodgson, Phys. Rev. B **67**, 174104 (2003).
[6] M. Haider, H. Rose, S. Uhlemann, B. Kabius, and K. Urban, J. Electron Microsc. **47**, 395 (1998).
[7] U. Weierstall, Q. Chen, J. C. H. Spence, M. R. Howells, M. Isaacson, and R. R. Panepucci, Ultramicroscopy **90**, 171 (2002).
[8] J. M. Zuo, I. Vartanyants, M. Gao, R. Zhang, and L. A. Nagahara, Science **300**, 1419 (2003).
[9] O. Kamimura, K. Kawahara, T. Doi, T. Dobashi, T. Abe, and K. Gohara, Appl. Phys. Lett. **92**, 024106 (2008).
[10] J. Yamasaki, H. Sawada, and N. Tanaka, J. Electron Microsc. **54**, 123 (2005).
[11] P. Hirsch, A. Howie, R. B. Nicholson, D. W. Pashley, and M. J. Whelan, *Electron Microscopy of Thin Crystals*, 2nd ed. (Krieger, Florida, 1977).
[12] S. Marchesini, H. He, H. N. Chapman, S. P. Hau-Riege, A. Noy, M. R. Howells, U. Weierstall, and J. C. H. Spence, Phys. Rev. B **68**, 140101 (2003).
[13] J. Miao, D. Sayre, and H. N. Chapman, J. Opt. Soc. Am. A **15**, 1662 (1998).
[14] J. R. Fienup, J. Opt. Soc. Am. A **4**, 118 (1987).
[15] I. A. Vartanyants and I. K. Robinson, J. Phys.: Condens. Matter **13**, 10593 (2001).
[16] J. C. H. Spence, U. Weierstall, and M. Howells, Ultramicroscopy **101**, 149 (2004).
[17] C. Dwyer, A. I. Kirkland, P. Hartel, H. Muller, and M. Haider, Appl. Phys. Lett. **90**, 151104 (2007).
[18] B. Freitag, J. Stanley, E. Sourty, J. Ringnalda, and D. Hubert, Microsc. Microanal. **13**, 834 (2007).